Novel *N,N′*-bis(2,4-dimethoxybenzylidene)-ethylenediamine PVC membrane electrode for the potentiometric iron selective sensor based on Schiff base ligand

Sachin Kumar[1), *)] (ORCID ID: 0000-0002-9131-582X), **Susheel K. Sandhu**[1)] (0000-0001-7944-8593), **Angik K. Patel**[2)] (0000-0001-6746-895X), **Ketankumar H. Parmar**[3)] (0000-0002-8886-7711)

DOI: dx.doi.org/10.14314/polimery.2022.5.2

Abstract: *N,N′*-bis(2,4-dimethoxybenzylidene)ethylenediamine was synthesized and used as a membrane carrier to create a novel poly(vinyl chloride) membrane potentiometric sensor that is selective especially for Fe^{3+} ions. The super-Nernstian slope of the projected sensor was 19.5 mV per decade over a concentration range of $7.3 \cdot 10^{-8}$–$1 \cdot 10^{-1}$ M having detection limit at $7.3 \cdot 10^{-8}$ M. The sensor displayed a linear potential response for the detection of Fe^{3+} ions in about 30 seconds, and it had a lifespan of no less than 9 weeks without lacking any potential divergence. The selected sensor showed high selectivity in water solutions in relation to Fe^{3+} ions, even in the presence of other metal cations in the pH range of 3.6–10.

Keywords: Fe^{3+} ions, ion-selective electrode, PVC membrane, potentiometry, Schiff base.

Nowa elektroda membranowa z PVC i *N,N′*-bis(2,4-dimetoksybenzylideno)-etylenodiaminy jako potencjometryczny jonoselektywny czujnik żelaza oparty na ligandzie zasady Schiffa

Streszczenie: Przedmiotem badań był potencjometryczny czujnik do selektywnego oznaczania jonów Fe^{3+} oparty na membranie wykonanej z poli(chlorku winylu) i *N,N′*-bis(2,4-dimetoksybenzylideno)etylenodiaminy. Nachylenie super-nernstowskie (ang. *super-Nernstian slop*) badanego czujnika wynosiło 9,5 mV na dekadę w zakresie stężeń $7,3 \cdot 10^{-8}$–$1 \cdot 10^{-1}$ M z limitem detekcji $7.3 \cdot 10^{-8}$ M. Czujnik wykazywał w obecności jonów Fe^{3+} liniową odpowiedź przez około 30 s, a jego czas życia bez rozbieżności potencjałów wynosił nie mniej niż 9 tygodni. Wybrany czujnik wykazywał w roztworach wodnych wysoką selektywność w stosunku do jonów Fe^{3+} nawet w obecności innych kationów metali w zakresie pH 3,6–10.

Słowa kluczowe: jony Fe^{3+}, elektrody jonoselektywne, membrana PVC, potencjometria, zasada Schiffa.

Iron is the universe's sixth most prevalent fundamental element. It is one of the most abundant trace minerals found in the human body for energy production. As a result, iron is a necessary component of biological systems, as it is involved in electron transport, oxygen transport, and storage [1, 2]. Iron is found in the basic structures of haemoglobin, myoglobin, hem ases, and a variety of cofactors that are required for enzyme action. Anemia, which is caused by iron deficiency, poses a health risk to humans. The liver and kidneys are harmed when there is too much iron in the body (hemochromatosis). Some iron compounds are linked to the development of cancer [3]. Excess iron, on the other hand, can lead to a variety of health issues. High iron levels, for example, raise the risk of cancer, heart disease, and other disorders including hemochromatosis [4]. Atomic absorption spectroscopy (AAS), catalytic spectrophotometric injection analysis, and other approaches for iron ion measurement have been proposed in clinical, pharmaceutical, environmental, and industrial settings [5], colorimetry [6], spectrophotometry [7], liquid-liquid microextraction [8], and inductively coupled plasma (ICP). These techniques are used to determine trace levels of iron [9, 10]. They do, however, have drawbacks, such as a high cost and inability to be used for routine analysis. Ion-selective sensors (ISEs) are potentiometric sensors that are simple to use, affordable, provide quick responses with a good dynamic concentration range and detection limit, and can be easily applied to real samples,

---

[1)] Department of Chemistry, S.S.V.P.G. College (Affiliated to C.C.S. University Meerut, Meerut), Hapur-245101, India.

[2)] Department of Chemistry, Mahisagar Science College, Lucknow, India.

[3)] Department of Chemistry, Navjivan Science College, Dahod-389150, India.

[*)] Author for correspondence: singhsachin001990@gmail.com

making them a simple, quick, and dependable tool [11]. As a result, they can be considered as a useful instrument for finding the concentration of a certain ionic target in the occurrence of intrusive ionic species in the aqueous medium [12]. However, just a few Fe^{3+}-selective sensors can be identified as a simple, quick, and reliable analytical tool [13–16]. Some of these electrodes are made of chalcogenide glass, while others are made of plasticized polymers [17]. Because of their peculiar and poorly known interfacial chemistry, the former ones are problematic. PVC-based sensors are preferred because their composition may be optimized to achieve good selectivity. ISEs have sparked a lot of interest in the sectors of environmental, agricultural, and industrial analysis due to their multiple advantages, such as ease of synthesis and applications, high stability with good specificity, and quick response [18–20].

New ionophore for Fe^{3+} sensor manufacturing is still desirable because the earlier stated sensors are not yet exceptionally selective and sensitive. Because Schiff bases are known to form strong complexes along with the ions of transition metals, they are an important class of chemicals that can be used for this purpose [21]. While much effort was done on the production of crystal structure and characterization of metal-salen complexes, only a few salen molecules were employed as ionophore in ISEs [22]. Mashhadizadeh *et al.* [23] described an iron-selective electrode created on a Schiff base, but the electrode produced a super-Nernstian response. As a result, we investigated the feasibility of employing Schiff base as an ionophore in the construction of Fe^{3+} sensors. We investigated a number of Schiff bases mentioned in the reported literature as ionophores for constructing Fe^{3+}-selective sensors for this purpose. Our findings show that a PVC-based membrane containing -bis(tridentate) ligand works as a good Fe^{3+} sensor, and findings are presented in this paper. We presented a PVC-based, highly Fe^{3+}-selective sensor for the potentiometric detection of Fe^{3+} ions over a wide-ranging concentration, using *N,N′*-bis(2,4-dimethoxybenzylidene)ethylenediamine Schiff base as the ionophore.

EXPERIMENTAL PART

Materials

All chemicals and reagents used were of high pure analytical reagent (AI) grade. Reagent grade dioctyl phthalate (DOP), sodium tetraphenyl borate (NaTPB) purchased from Fluka, dibutyl phthalate (DBP) and tetrahydrofuran (THF) purchased from Alfa Aegear, iron(III) nitrate $Fe(NO_3)_3$, and high relative molecular weight poly(vinyl chloride) (PVC) were purchased from Sigma-Aldrich. 1-chloronaphthalene (CN) and *o*-nitrophenyl octyl ether (*o*-NPOE) were supplied from Merck. 2,4-dimethoxybenzaldehyde ($C_9H_{10}O_3$) and ethylenediamine ($C_2H_4(NH_2)_2$) purchased from Merck and BDH respectively were reagent grade materials. All the reagents were used as received. $1{\cdot}10^{-1}$ M stock solution of metals was prepared by using double distilled water and further more diluted to prepare various solution concentrations.

Synthesis of *N,N′*-bis(2,4-dimethoxybenzylidene)-ethylenediamine ionophore

N,N′-bis(2,4-dimethoxybenzylidene)ethylenediamine was synthesized as follows: a hot ethanolic solution, 20 ml of ethylenediamine and 2,4-dimethoxybenzaldehyde (1 g, 6 mmol) were mixed together under steady stirring. The chemical fusion reaction was re-fluxed for about 3 hours at 40–45°C. After freezing for an hour, a white powder was separated, filtered, washed, and recrystallized with 50% ethanol before overnight vacuum drying. The chemical structure of *N,N′*-bis(2,4-dimethoxybenzylidene)ethylenediamine and its synthesis are shown in Scheme 1.

The reaction yield was 83.27% and melting point ~159.03°C. 1H NMR δH ($CDCl_3$): 3.84 (s, 3H, OCH_3), 3.86 (s, 3H, OCH_3), 3.89 (s, 2H, $-CH_2-N=$), 6.46 (s, 1H, HdAr), 6.55 (d, 1H, HbAr), 7.26 (s, 1H, HaAr), 7.89 (s, 1H, HcAr), and 8.67 (s, 1H, -CH=N-). IR (KBr disk, cm^{-1}): ν(C-O) 537, 576, 832, 1033, ν(C-N) 1128, 1169, ν(C-C) 1207, 1267, ν(C=C) 1424, 1468, 1506, 1609, ν(-CH=N-) 1639, ν(C-H, Ar) 2837, ν(C-H, Me) 2884, 2997. UV-Vis, λ_{max} ($CHCl_3$): 278 nm, 325 nm. Analysis of ligand (L) calculated: C 72.36%, H 4.98%, N 10.78%, measured: C 65.78%, H 6.59%, N 7.69%.

Synthesis of PVC membrane electrode in four different compositions

PVC-based membrane was made according to the typical technique described previously [23]. Different composition of membrane ingredients, including ionophore, anionic additives (NaTPB and PVC), and 4 different plasticizers, namely *o*-nitrophenyl octyl ether (*o*-NPOE), dibutyl phthalate (DBP), dioctyl phthalate (DOP), and 1-chloronaphthalene (CN) [24, 25], were thoroughly dissolved in 5 ml of tetrahydrofuran (THF) as shown in Table 1.

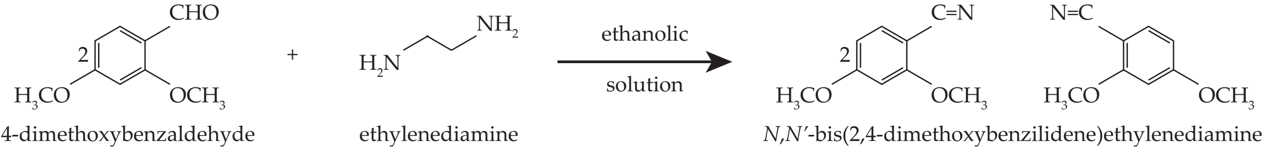

Scheme 1. Reaction scheme for the preparation of *N,N′*-bis(2,4-dimethoxybenzylidene)ethylenediamine

After complete dissolving, solution was dispensed into acrylic rings positioned on a plane glass dish. The mixture was allowed to evaporate for 20 to 24 hours at ambient conditions, giving clear membranes with a thickness of roughly ~0.1 mm. These membranes were once again cut into 5 mm diameter spherical shaped discs and attached with araldite glue to one end of a pyrex glass tube. Membrane materials ratio, time of contact, and equilibrating fluid concentration were all especially selected to generate reproducible and stable potentials. Optimal fabrication conditions ensured membrane-to-membrane repeatability. For additional research, membrane with the most consistent results and best performance was chosen. When not in use, membranes were maintained in a 0.1 M salt solution to prevent dehydrating, cracking, and harming.

Methodology

Membrane conditioning and electrode potential measurements

The membranes were homogenized in 1 M $Fe(NO_3)_3$ aqueous solutions for three days. The membrane potentials were measured throughout a wide range of concentration of the tested solution, *i.e.*, $1{\cdot}10^{-8}$–$1{\cdot}10^{-1}$ M. The typical $Fe(NO_3)_3$ solutions were made by gradually diluting a $Fe(NO_3)_3$ $1{\cdot}10^{-1}$ M solution. The electrochemical setup described below was used to measure electrode potential (EMF), at 25°C.

Ag/AgCl | KCl (std.) | 0.1 M $Fe(NO_3)_3$ || PVC membrane || test solution | Ag/AgCl | KCl (std.)

An inner reference solution of 0.1 M $Fe(NO_3)_3$ was used. The EMFs of the tested solutions were measured for concentrations from high ($1{\cdot}10^{-1}$ M) to low ($1{\cdot}10^{-8}$ M) to determine electrode performance. The Fe^{3+} ion activity coefficients were estimated using the modified Debye-Hückel technique and the following Equation (1):

$$\log \gamma = (-0.511z^2)[\mu^{1/2}/(1+ 1.5\ \mu^{1/2}) - 0.2\mu] \tag{1}$$

where:
γ – activity coefficient
μ – ionic strength
z – ion charge.

pH measurements

Glass and calomel pH electrodes were used as reference electrode respectively. The electrodes pH dependency was evaluated by measuring the potential response of a Fe^{3+} $1{\cdot}10^{-3}$ M ion solution in the range from 1 to 13. HCl (0.1 M) and NaOH solutions were used to adjust pH. Esico International Digital Potentiometer Model-118 was used to detect potential at 25°C with a pH/mV meter using the projected sensor in conjugation with an Ag/AgCl as reference electrode. pH was measured by a digital pH-meter (Esico International Digital pH-meter Model-101).

Determination of ion selectivity

In the presented study, fixed interference method (FIM), recommended by IUPAC, was used to calculate the selectivity coefficients. The potentials of mixtures of intrusive ion ($a_B = 1{\cdot}10^{-2}$ M) with primary Fe^{3+} ion solutions which concentrations ranged between $1{\cdot}10^{-8}$ M to $1{\cdot}10^{-1}$ M were measured.

The major ion's activity was plotted against the observed potential levels. Using Equation (2), the coefficients of potentiometric selectivity were graphically computed [2].

$$K_{Fe,B}^{Pot} = \frac{a_{Fe^{3+}}}{(a_B)^{Z_{Fe}}_{Z_{Fe}Z_B}} \tag{2}$$

where:
$a_{Fe^{3+}}$ – activity of the primary ion
a_B – activity of the interfering ion
$Z_{Fe}Z_B$ – charges on the primary and interfering ions.

RESULTS AND DISCUSSION

Potential response study and optimization of membrane composition

The working idea of PVC-based membranes is that the integrated carrier preferentially recognizes the analyte ion by forming a compound with it [26]. The *N,N'*-bis(2,4-dimethoxybenzylidene)ethylenediamine as ligand (L) forms strong complexes with Fe^{3+} ions, according to a recent work [27]. To achieve stable potentials, heterogeneous membranes were manufactured in this study using the aforementioned ligand and a PVC matrix in various ratios, and the membranes were homogenized in 0.5 M Fe^{3+} ion solution for about 3 days. The membrane sensors' potentiometric response properties were tested under the following conditions: the Fe^{3+} concentration of the testing solution was between $1{\cdot}10^{-8}$ M and $1{\cdot}10^{-1}$ M with the internal solution concentration set at $1{\cdot}10^{-2}$ M. As shown in Fig. 1, the potential responses of the most common cations (Cu, Cd, Co, Zn, Ni, K, Na, Pb, Fe, Ba, Mn, Ca, Al) were plotted against the logarithm of Fe^{3+} activity. In most cases, the inclination of the corresponding potential was much lower than 59.5 mV and 29.5 mV per decade for monovalent and divalent anions, respectively (save for the iron ion-selective membrane electrode). The influence of membrane composition, type of plasticizer and its amount, and lipophilic additive NaTPB on the potential response of the suggested Fe^{3+} sensor with various metal ions was examined. Table 1, Fig. 1, and Fig. 2 summarize the results. Sensor 1 was a membrane that contained only ligand and anion excluder NaTPB in PVC matrix in a 5 : 75 : 2 ratio

Table 1. Composition and response characteristics of Schiff base ligand membrane

Sensor number	Membrane composition (w/w)				Working concentration range, M	Slope mV/decade of activity	Response time
	Ionophore	PVC	Plasticizer	NaTPB			
1	5	75	0	2	$1 \cdot 10^{-5}$–$1 \cdot 10^{-1}$	30.5±0.1	55
2	5	75	100 (CN)	2	$5 \cdot 10^{-6}$–$1 \cdot 10^{-1}$	13.2±0.2	35
3	5	75	100 (DOP)	2	$1 \cdot 10^{-6}$–$1 \cdot 10^{-1}$	25.6±0.1	42
4	5	75	100 (*o*-NPOE)	2	$7.3 \cdot 10^{-8}$–$1 \cdot 10^{-1}$	19.5±0.3	30
5	5	75	100 (DBP)	2	$1.9 \cdot 10^{-5}$–$1 \cdot 10^{-1}$	32.0±0.4	25

(ligand : PVC : NaTPB measured in w/w, mg). Its operating concentration range was $1 \cdot 10^{-5}$–$1 \cdot 10^{-1}$ M of Fe^{3+}. Its super-Nernstian slope per decade of activity was 30.5±0.1 mV. Plasticizers used in the manufacture of ion-selective electrodes had an impact on their selectivity and sensitivity (ISEs).

As a result, several membranes were doped with various 4 plasticizers, such as DOP, DBP, CN, and *o*-NPOE, and the response characteristics of these doped membranes were examined to see how these plasticizers affect the response. Table 1 shows the optimal composition and response characteristics of these membranes, which are represented in Fig. 1.

Plasticizers, with the exception of DOP, significantly enhanced the operating concentration range of the sensors, as seen in Fig. 1 and Table 1. The working concentration range was widened by the addition of CN, *o*-NPOE, and DBP to $5 \cdot 10^{-6}$–$1 \cdot 10^{-1}$ M, $7.3 \cdot 10^{-8}$–$1 \cdot 10^{-1}$ M, and $1.9 \cdot 10^{-5}$–$1 \cdot 10^{-1}$ M, respectively. However, addition of DOP had no effect on the working concentration range. The limit of detection for sensor 4 was determined by intersecting two extrapolated portions of the calibration curve (Fig. 3), and it was determined to be $7.5 \cdot 10^{-8}$ M. The results were significantly better after addition of *o*-NPOE and DBP whereas on observing the results we can conclude that *o*-NPOE have higher polarity and lipophilicity as compared to DBP. Sensor 4 with plasticizer *o*-NPOE was chosen for all further studies based on the aforementioned response characteristics of all evaluated electrodes.

Dynamic response time and lifetime analysis

The response speed of the sensor determines how useful it is in batch observations and flow networks. The dynamic reaction time is a periodic record of the response that may be easily generated from the original conditioning in the supporting solution with incremental concentration additions spanning several orders of magnitude [28]. The suggested membrane sensor's dynamic response time is shown in Fig. 4 and listed in Table 1. The suggested sensor's reaction time was 30 s, as shown in Fig. 4 (sensor 4).

The suggested Fe^{3+} sensor's lifetime was assessed and verified for 10–12 weeks, through which sensors were heavily used for one hour in a week. Fig. 5 depicts the acquired results. The substantial alterations in the slope of the Fe^{3+} sensor occurred at 9th week, as expected. As a result, the suggested Fe^{3+} sensor could be operated for at least 9 weeks without making any noticeable divergence. The lifetime of the sensor was calculated by executing periodic calibrations with standard solutions and computing the response and gradient over the concentration range $1 \cdot 10^{-6}$ M to $1 \cdot 10^{-1}$ M of Fe^{3+} solution. The sensor per-

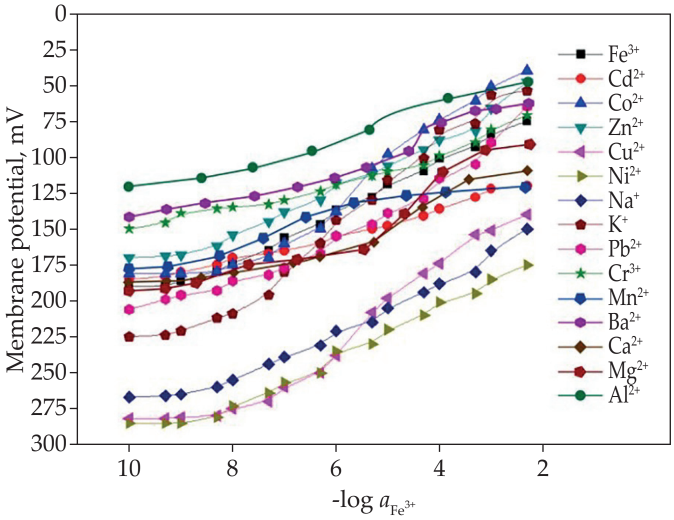

Fig. 1. Anion-selective electrodes potential response

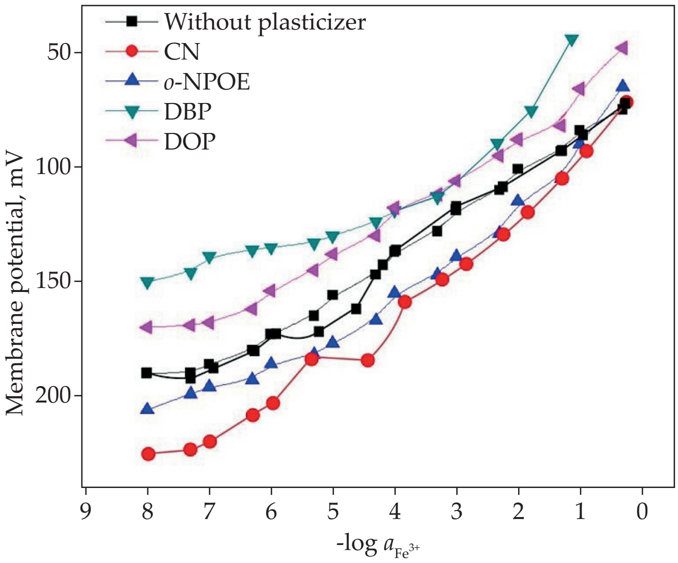

Fig. 2. Membrane potential variation of PVC-based membranes with different concentration of Fe^{3+} ions

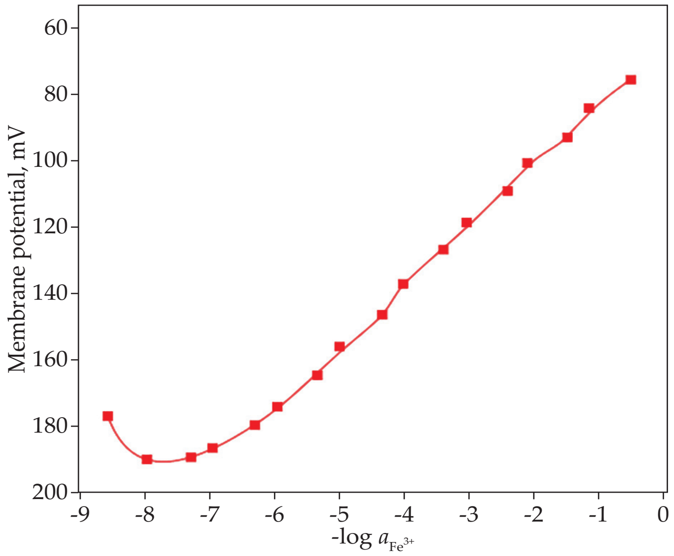

Fig. 3. Calibration plot for Fe^{3+} ion-selective sensor 4

formed well during a 9-week period, with strong repeatability and a standard deviation of ±0.1 mV in detected potential values in the working concentration range.

Effect of pH change

The stimulus of pH on the membrane electrode was considered in this study by examining its potential response for Fe^{3+} ion in two fixed concentrations, $1{\cdot}10^{-2}$ M and $1{\cdot}10^{-3}$ M, as shown in Fig. 6. The pH of tested solution was changed using diluted hydrochloric acid or sodium hydroxide (HCl/NaOH) to determine the operational range. The potentials of sensor 4 based on ligand remained constant in the pH range of 3–10, as shown in Fig. 6. The results revealed that the electrode potential was unaffected by the pH of the solution in the range of 3–10, which could be considered working and practical pH range of the chosen electrode. The change in potential below pH = 3 could be due to interference from hydrogen ions (H^+), which actively participated in the membrane's charge transport mechanism, while the alteration in potential above pH~10 could be due to intense iron ion (Fe^{3+}) hydrolysis.

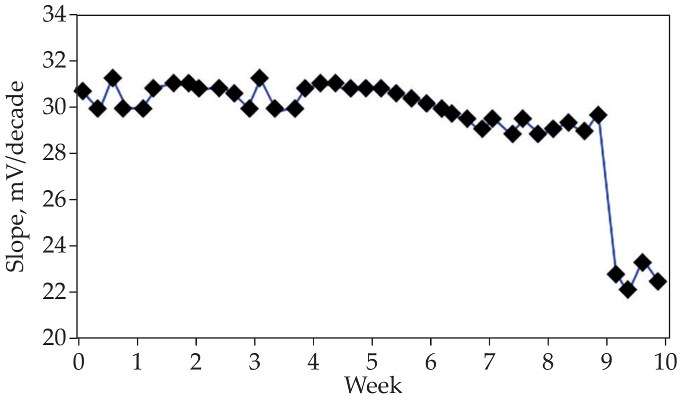

Fig. 5. Lifetime of the suggested sensor

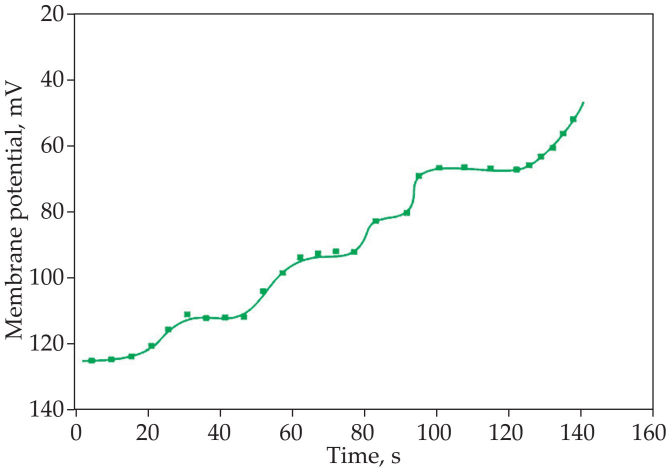

Fig. 4. Dynamic response time of optimized Fe^{3+}-selective sensor for step changes in concentrations of Fe^{3+}

Potentiometric selectivity

The most significant feature of ion-selective electrodes (ISEs) is their selectivity. Selectivity determines the nature of the device and the working concentration range in which it can be used successfully. The potentiometric selectivity coefficient ($K^{\mathrm{Pot}}_{\mathrm{A,B}}$) was used to calculate selectivity. The fixed interference method (FIM) was used to estimate the potentiometric selectivity coefficient in the presented study, with the modified form of the Nicolsky Equation (3):

$$K^{\mathrm{Pot}}_{\mathrm{A,B}} = \frac{\Delta a_{\mathrm{A}}}{a_{\mathrm{B}}} \tag{3}$$

where:
a_{A} – activity of the primary ion
a_{B} – activity of interfering ions (concentration $1{\cdot}10^{-2}$ M).

The selectivity coefficients determined for the sensors based on two ionophores are summarized in Table 2. As can be observed, the electrode responded selectively to Fe^{3+} ions. The membrane responds equally to the major

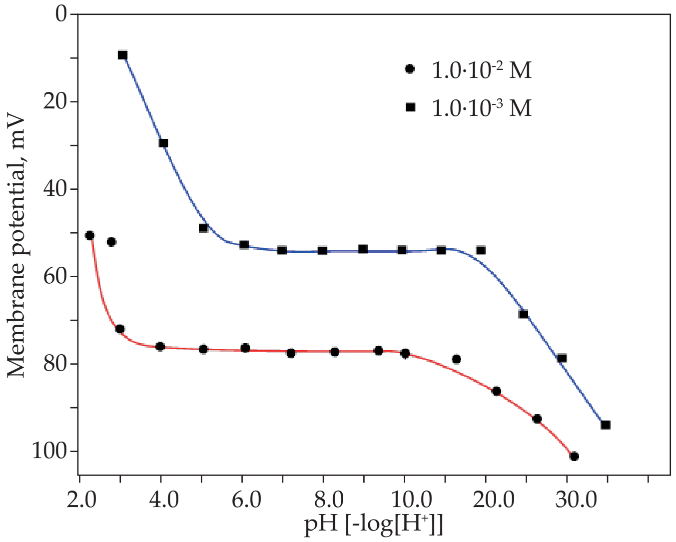

Fig. 6. Effect of pH of tested solution on the potential response of Fe^{3+} ion-selective electrode

T a b l e 2. Selectivity coefficients of Fe^{3+} ion-selective electrode

Interfering ion (B)	Selectivity coefficient ($\log K^{\text{Pot}}_{\text{A,B}}$)
Cu^{2+}	$4.7\cdot10^{-2}$
Cd^{2+}	$3.0\cdot10^{-3}$
Co^{2+}	$3.8\cdot10^{-3}$
Zn^{2+}	$3.4\cdot10^{-3}$
Ni^{2+}	$3.3\cdot10^{-3}$
K^{+}	$4.0\cdot10^{-2}$
Na^{+}	$4.2\cdot10^{-2}$
Pb^{2+}	$3.5\cdot10^{-3}$
Fe^{3+}	$3.2\cdot10^{-3}$
Ba^{2+}	$3.0\cdot10^{-3}$
Mn^{2+}	$2.5\cdot10^{-2}$
Ca^{2+}	$3.1\cdot10^{-2}$
Mg^{2+}	$3.1\cdot10^{-3}$
Al^{3+}	$4.2\cdot10^{-4}$

and interfering ions when the selectivity coefficient is 1.0. In this circumstance, a value ≤1.0 indicates that the electrode responds more to primary ion than interfering ion, and the electrode is deemed selective to primary ion over interfering ion. The table shows that selectivity coefficients for practically all of the tested ions were in the order of 10^{-2} and 10^{-3} or lower. These ions would not produce any significant interference in the estimation of Fe^{3+} ions with the suggested electrode unless they were present in large numbers.

The electroactive substance in the membrane was ionophore, which facilitated only ion transport, hence the membrane responded only to ions. Because organic compounds couldn't pass through the membrane, they would not cause any impact, as shown in Table 2. As a result, the suggested sensor was clearly selective for Fe^{3+} ions throughout a wide range of monovalent, divalent, and trivalent cations. It is sufficiently selective over these ions, allowing direct potentiometry to be used in estimation of iron ions in the presence of all these ions.

Effect of non-aqueous solvents

Non-aqueous material may be present in real samples. The research focused on the operation of the suggested sensor in partially non-aqueous mixtures of methanol-water, ethanol-water, and acetonitrile-water at concentrations of 10, 15, 20, and 25% (v/v). The results are summarized in Table 3. In mixtures containing up to 20% (v/v) of non-aqueous content, the sensor's working concentration range and slope did not vary significantly. However, in combinations with a non-aqueous content of 25% or more, both the working concentration range and slope of potentials were changing in time. This is most likely due to ionophore leaching with increasing of organic content.

ANALYTICAL APPLICATIONS

Potentiometer titration with EDTA

The sensor's use as an pointer electrode for potentiometric titration of Fe^{3+} ion solution was also evaluated in this work. 25 ml of $1\cdot10^{-2}$ M $Fe(NO_3)_3$ was titrated against $1\cdot10^{-2}$ M EDTA solution. The pH of the solution was kept at 4 during the titration with the use of diluted HCl and NaOH. The titration plot at pH 4 had normal sigmoidal shape, as illustrated in Fig. 7. As could be observed, the electrode properly estimated the amount of iron ions in solution. The measured potential revealed an unusual logarithmic variation with the titrant amount (in ml) added before the titration endpoint, whereas the potential response after the endpoint would remain constant

T a b l e 3. Effect of partially non-aqueous medium on Fe^{3+} sensor

Solvent	Non-aqueous content % (v/v)	Working concentration M	Slope mV/decade of a_{Fe}^{3+}
No solvent	0	$1\cdot10^{-1}$–$7.8\cdot10^{-8}$	20.4
Methanol	10	$1\cdot10^{-1}$–$7.8\cdot10^{-8}$	20.0
	15	$1\cdot10^{-1}$–$7.8\cdot10^{-8}$	20.0
	20	$1\cdot10^{-1}$–$7.7\cdot10^{-8}$	20.1
	25	$1\cdot10^{-1}$–$5.8\cdot10^{-6}$	20.4
Ethanol	10	$1\cdot10^{-1}$–$7.9\cdot10^{-8}$	20.0
	15	$1\cdot10^{-1}$–$7.8\cdot10^{-8}$	20.0
	20	$1\cdot10^{-1}$–$7.7\cdot10^{-8}$	20.0
	25	$1\cdot10^{-1}$–$5.9\cdot10^{-6}$	28.4
Acetonitrile	10	$1\cdot10^{-1}$–$7.8\cdot10^{-8}$	20.0
	15	$1\cdot10^{-1}$–$7.8\cdot10^{-8}$	20.0
	20	$1\cdot10^{-1}$–$7.7\cdot10^{-8}$	20.3
	25	$1\cdot10^{-1}$–$5.9\cdot10^{-6}$	29.5

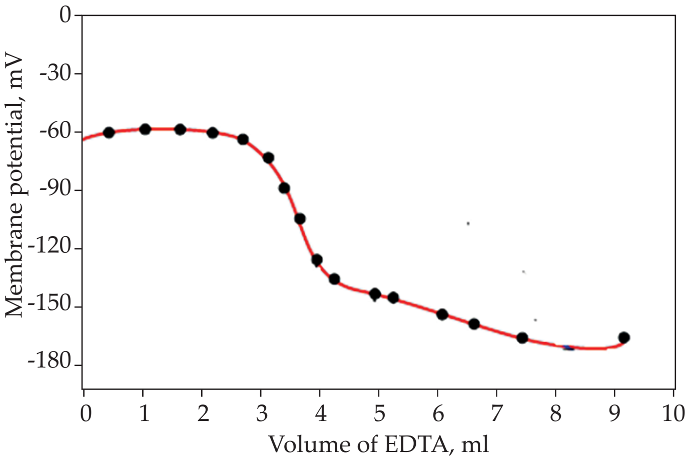

Fig. 7. Potentiometric titration curve of $1\cdot10^{-2}$ M Fe^{3+} with $1\cdot10^{-2}$ M EDTA solution using the suggested sensor 4 at pH 4

due to the low concentration and minor changes of free Fe^{3+} ions in solution. The concentration of Fe^{3+} ions was reduced after EDTA addition, resulting in a decrease of line potential. The breakpoint, on the other hand, was acute and corresponded to the Fe^{3+}-EDTA complex's 1 : 1 stoichiometry. Research showed, that the electrode assembly could be used to determine Fe^{3+} ions via potentiometric titration.

Determination of Fe^{3+} ions in real water samples

Under laboratory conditions only, the efficacy of the suggested sensor was further explored to determine Fe^{3+} ions in real samples of water categorized into three types: (a) pure mineral, (b) contaminated waste, and (c) flowing river water. Because of the low concentration and small variation of free Fe^{3+} ions in solution, the measured potential changed in an atypical logarithmic manner with the titrant amount (in ml) added before the titration endpoint, whereas the potential response after the endpoint was nearly constant. The % recovery rate for Fe^{3+} was found to be in good agreement between spiking and measured analyte levels, as showed in Table 4. The examined sensor's results were in good agreement with those of atomic absorption spectroscopy (AAS). As a result, the suggested sensor may be successfully used to determine iron in real samples, and it had the following benefits: high accuracy, simplicity, colored solutions, turbidity adaptation, low cost, quality control of ionophore formulations, automation, and speed.

Comparative analysis

Table 5 presents the comparison of our suggested sensor with previously reported ones in terms of their reported working concentration, detection limit, slope, response time, and pH range.

CONCLUSION

The *N,N′*-bis(2,4-dimethoxybenzylidene)ethylenediamine ligand (L) was used to design a potentiometric PVC-based membrane sensor. This research found that in the concentration range of $7.3\cdot10^{-8}$ M to $1\cdot10^{-1}$ M this membrane sensor performed very well as a Fe^{3+} ion-selective membrane sensor with Nernstian behavior (19.5 mV/decade). The sensor had a quick response

Table 4. Determination of Fe^{3+} ions in different water samples

Water sample	Suggested sensor, mg/l	AAS, mg/l	Recovery, %
Mineral water 1	1.64±0.2	1.82±0.4	97.2
Mineral water 2	1.83±0.2	1.54±0.3	97.8
Contaminated water 1	4.54±0.3	4.11±0.2	96.3
Contaminated water 2	4.73±0.4	4.54±0.3	97.2
River water 1	1.72±0.3	1.50±0.2	97.4
River water 2	2.40±0.2	2.30±0.4	98.9

Table 5. Comparison of characteristics of suggested Fe^{3+} ion-selective sensor with other Fe^{3+} ion-selective sensors

Ionophore	Working concentration range, M	Detection limit, M	Slope mV/decade	Response time, s	pH range	Reference
2-methyl-6-(4- methylenecyclohex-2-en-1--yl)-hept-2-en-4-one (MMCHH)	$4.3\cdot10^{-7}$–$1\cdot10^{-2}$	$4.3\cdot10^{-7}$	19.3±0.5	10	1.5–6	[29]
benzo-18crown-6 (b-18C6)	$1\cdot10^{-6}$–$1\cdot10^{-1}$	$8\cdot10^{-7}$	19.5±0.1	12	2.5–5.7	[30]
μ-bis(tridentate)	$6.3\cdot10^{-6}$–$1\cdot10^{-1}$	$5\cdot10^{-6}$	20	15	3.5–5.5	[20]
N-(2-hydroxyethyl)ethylenediamine-*N, N′, N″*-triacetic acid (NTA)	$1\cdot10^{-9}$–$1\cdot10^{-2}$	$3\cdot10^{-10}$	19.5±0.4	10	1.8–4.5	[31]
N,N′-bis(2,4-dimethoxybenzylidene)-ethylenediamine	$7.3\cdot10^{-8}$–$1\cdot10^{-1}$	$7.5\cdot10^{-8}$	19.5±0.3	9	3.6–10	Presented study

time of 30 seconds over the full concentration range and could be used to determine Fe^{3+} ions in the presence of common interfering ions at high concentrations. The detection limit of the electrode was $7.5 \cdot 10^{-8}$ M. The suggested sensor is suitable for Fe^{3+} determination due to its pH range, lower detection limit, and potentiometric selectivity coefficients.

REFERENCES

[1] Goyer R.A., Clarkson T.W.: "The Basic Science of Poisons" Ch. 23 "Toxic Effects Of Metals", Ed. 5, McGraw-Hill, New York City NY, 1996, 812. https://www.biologicaldiversity.org/campaigns/get_the_lead_out/pdfs/health/Goyer_1996.pdf

[2] Greentree W.F., Hall J.O.: "Kirk's Current Therapy XII Small Animal Practice", Bonagura J.D. (Eds.), WB Saunders Co., Philadelphia PA, 1995, 240. https://pubs.er.usgs.gov/publication/5224770

[3] Neirz M., Weiss G.: *Molecular Aspects of Medicine* **2020**, *75*, 100864. https://doi.org/10.1016/j.mam.2020.100864

[4] Tang B., Zhang L., Geng Y.: *Talanta* **2005**, *65*, 769. https://doi.org/10.1016/j.talanta.2004.08.004

[5] Lunvongsa S., Oshima M., Motomizu S.: *Talanta* **2006**, *68*, 969. https://doi.org/10.1016/j.talanta.2005.06.067

[6] Masawat P., Harfeld A., Srihirun N. *et al.*: *Analytical Letters* **2017**, *50*, 173. https://doi.org/10.1080/00032719.2016.1174869

[7] Samadi A., Amjadi M.: *Journal of Applied Spectroscopy* **2016,** *83*, 422. https://doi.org/10.1007/s10812-016-0304-3

[8] Peng B., Chen G., Li K. *et al.*: *Food Chemistry* **2017**, *230*, 667. https://doi.org/10.1016/j.foodchem.2017.03.099

[9] Pooyamanesh M.J., Zamani H.A., Rajabzadeh G. *et al.*: *Analytical Letters* **2007**, *40*, 1596. https://doi.org/10.1080/00032710701380632

[10] Peng B., Shen Y., Gao Z. *et al.*: *Food Chemistry* **2015**, *176*, 288. https://doi.org/10.1016/j.foodchem.2014.12.084

[11] Balderas-Hernández P., Roa-Morales G., Ramírez--Silva M.T. *et al.*: *Chemosphere* **2017**, *167*, 314. https://doi.org/10.1016/j.chemosphere.2016.10.009

[12] Shen J., Gagliardi S., McCoustra M.R.S. *et al.*: *Chemosphere* **2016**, *159*, 66. https://doi.org/10.1016/j.chemosphere.2016.05.069

[13] Zamani H.A., Shoshtari M., Feizyzadeh B.: *International Journal of Electrochemical Science* **2015**, *10*, 8644. http://www.electrochemsci.org/papers/vol10/101008644.pdf

[14] Zamani H.A., Ganjali M.R., Faridbod F. *et al.*: *Materials Science and Engineering: C* **2012**, *32*, 564. https://doi.org/10.1016/j.msec.2011.12.009

[15] Alizadeh K., Parooi R., Hashemi P. *et al.*: *Journal of Hazardous Materials* **2011**, *186*, 1794. https://doi.org/10.1016/j.jhazmat.2010.12.067

[16] Zamani H.A., Imani A., Arvinfar A. *et al.*: *Materials Science and Engineering: C* **2011**, *31*, 588. https://doi.org/10.1016/j.msec.2010.11.016

[17] Enseleit U., Feller C., Partsch U. *et al.*: *Journal of Solid State Electrochemistry* **2021**, *25*, 2293. https://doi.org/10.1007/s10008-021-05000-1

[18] Lindfors T., Sundfors F., Höfler L. *et al.*: *Electroanalysis* **2011**, *23*, 2156. https://doi.org/10.1002/elan.201100219

[19] Zamani H.A., Ganjali M.R., Salavati-Niasari M.: *Transition Metal Chemistry* **2008**, *33*, 995. https://doi.org/10.1007/s11243-008-9142-3

[20] Farzad D.: *Talanta* **1999**, *50*, 1129. https://doi.org/10.1016/S0039-9140(99)00194-0

[21] Kumar S., Mittal S.K., Kaur N. *et al.*: *RSC Advances* **2017**, *7*, 16474. https://doi.org/10.1039/C7RA00393E

[22] Gualandi A., Calogero F., Potenti S. *et al.*: *Molecules* **2019**, *24*, 1716. https://doi.org/10.3390/molecules24091716

[23] Mashhadizadeh M.H., Shoaei I.S., Monadi N.: *Talanta* **2004**, *64*, 1048. https://doi.org/10.1016/j.talanta.2004.05.005

[24] Kumar S., Sindhu S.K., Kumar P. *et al.*: *Polimery* **2021**, *66*, 589. https://doi.org/10.14314/polimery.2021.11.4

[25] Mashhadizadeh M.H., Momeni A., Razavi R.: *Analytica Chimica Acta* **2002**, *462*, 245. https://doi.org/10.1016/S0003-2670(02)00309-4

[26] Umezawa Y., Umezawa K., Sato H.: *Pure and Applied Chemistry* **1995**, *67*, 507. https://doi.org/10.1351/pac199567030507

[27] Radfard R., Abedi A.: *Journal of Applied Chemistry Research* **2015**, *9*, 59. http://jacr.kiau.ac.ir/article_516079_84e4057aaab43e-a2bb678a9618cf459e.pdf

[28] Kazemi F., Zamani H.A., Joz-Yarmohammadi F. *et al.*: *Bulgarian Chemical Communications* **2017**, *49*, 449. http://bcc.bas.bg/BCC_Volumes/Volume_49_Number_2_2017/49-2-2017-4220-Kazemi-449-454.pdf

[29] Badakhshan S., Ahmadzadeh S., Mohseni-Bandpei A. *et al.*: *BMC Chemistry* **2019**, *13*, ID 131. https://doi.org/10.1186/s13065-019-0648-x

[30] Gupta V.K., Jain A.K., Agarwal S. *et al.*: *Talanta* **2007**, *71*, 1964. https://doi.org/10.1016/j.talanta.2006.08.038

[31] Zamani H.A., Hamed-Mosavian M.T., Hamidfar E. *et al.*: *Materials Science and Engineering: C* **2008**, *28*, 1551. https://doi.org/10.1016/j.msec.2008.04.013

Received 10 II 2022.